Nutritional Control of Elongation of DNA Replication by (p)ppGpp

Jue D. Wang,[1,3] Glenn M. Sanders,[2] and Alan D. Grossman[1,*]

[1] Department of Biology, Building 68-530, Massachusetts Institute of Technology, Cambridge, MA 02139, USA
[2] Replidyne, Inc., Louisville, CO 80027, USA
[3] Present address: Department of Molecular and Human Genetics, Baylor College of Medicine, One Baylor Plaza, Room S-911, Houston, TX 77030, USA.
*Correspondence: adg@mit.edu

SUMMARY

DNA replication is highly regulated in most organisms. Although much research has focused on mechanisms that regulate initiation of replication, mechanisms that regulate elongation of replication are less well understood. We characterized a mechanism that regulates replication elongation in the bacterium *Bacillus subtilis*. Replication elongation was inhibited within minutes after amino acid starvation, regardless of where the replication forks were located on the chromosome. We found that small nucleotides ppGpp and pppGpp, which are induced upon starvation, appeared to inhibit replication directly by inhibiting primase, an essential component of the replication machinery. The replication forks arrested with (p)ppGpp did not recruit the recombination protein RecA, indicating that the forks are not disrupted. (p)ppGpp appear to be part of a surveillance mechanism that links nutrient availability to replication by rapidly inhibiting replication in starved cells, thereby preventing replication-fork disruption. This control may be important for cells to maintain genomic integrity.

INTRODUCTION

All organisms have mechanisms to duplicate and transmit DNA to progeny cells. DNA replication involves the action of >10 polypeptides and consists of initiation, elongation, and termination phases (Baker and Bell, 1998; Johnson and O'Donnell, 2005). Many bacteria, including *B. subtilis,* have a single circular chromosome (reviewed in Duggin and Wake, 2002; Lemon et al., 2002) with one origin of replication (*oriC*). During initiation, the replication machinery loads onto *oriC*. Elongation proceeds bidirectionally and duplicates the leading and lagging strands at each replication fork. In *B. subtilis,* termination occurs at *ter* sites, located approximately opposite from *oriC* (Figure 1A), by

the action of the replication-termination protein Rtp (Duggin and Wake, 2002).

Initiation of replication is coordinated with cell growth and division and is responsive to nutrient availability. The stringent response, a pleiotropic response to starvation (Cashel et al., 1996), contributes to regulation of replication initiation in response to amino acid starvation (Levine et al., 1991; Schreiber et al., 1995). The stringent response is triggered by amino acid starvation when RelA, a ribosome-bound enzyme, rapidly synthesizes the small nucleotides pppGpp (guanosine pentaphosphate) and ppGpp (guanosine tetraphosphate; together (p)ppGpp) from GTP and ATP. In *E. coli,* slow growth rates and nutritional downshifts inhibit replication initiation (Levine et al., 1991; Schreiber et al., 1995; Zyskind and Smith, 1992), and (p)ppGpp might contribute to this inhibition in part by decreasing transcription of *dnaA* (Zyskind and Smith, 1992), the gene for the replication initiation protein.

In *B. subtilis,* the stringent response regulates replication elongation. The stringent response can cause replication arrest ~100–200 kbp to the left and right of *oriC* (Figure 1A; Levine et al., 1991). It was proposed that Rtp binds to sites (called LSTer and RSTer) in these regions to mediate this arrest (Autret et al., 1999; Levine et al., 1995).

We found that the replication-elongation inhibition caused by the stringent response in *B. subtilis* occurs throughout the chromosome. This response occurs independently of previously proposed specific arrest sites near *oriC* and independently of Rtp. The response is mediated by the starvation signals (p)ppGpp, which appear to directly inhibit primase, an essential component of the replication complex. Regulation of replication elongation allows a much more rapid response to starvation than if replication were regulated at initiation alone.

Inhibition of replication elongation caused by a variety of adverse situations, including depletion of dNTPs or DNA damage, leads to arrest and disruption of replication forks, induction of the SOS response, and genomic instability (Michel et al., 2004 and references therein). We found that the replication forks arrested by (p)ppGpp did not detectably recruit RecA, indicating that the forks were probably not disrupted. We suggest that (p)ppGpp-mediated replication arrest contributes to the maintenance of genomic stability by preventing disruptive fork arrest that
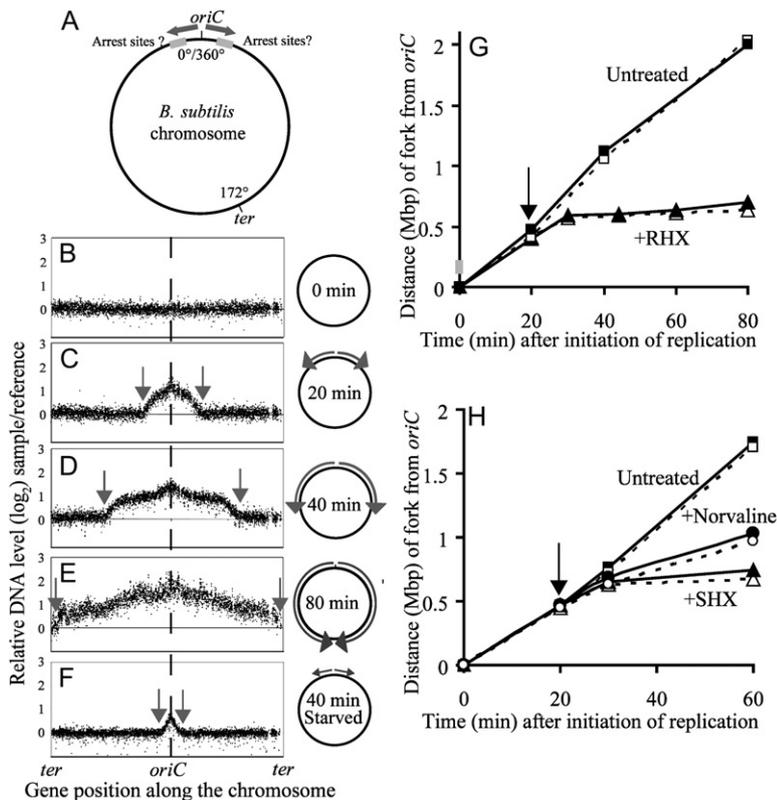
Figure 1. Monitoring Progression and Arrest of Replication Forks

(A) Diagram of the circular *B. subtilis* chromosome is shown. The origin (*oriC*) and terminus (*ter*) of replication, directions of fork progression (gray arrows), and regions (light gray bars) proposed to contain specific sites for replication arrest (Autret et al., 1999; Levine et al., 1991, 1995) are indicated.

(B–F) Replication in the *dnaBts* mutant (KPL69) was monitored using DNA microarrays to measure gene dosage throughout the chromosome. Relative DNA levels (log$_2$) were determined by cohybridization of replicating and preinitiation reference DNA to whole-genome microarrays, then plotted as a function of gene position. *oriC* is in the middle (0 Mbp), and *ter* is to the left ($\sim$−2.2 Mbp) and right ($\sim$2.0 Mbp). Arrows indicate the positions of the replication forks, which are defined as the boundaries between the replicated and unreplicated genes. Each panel shows data from one experiment and is representative of multiple experiments. Samples were taken immediately before (0 min; B) and 20 (C), 40 (D), and 80 min (E) after initiation of replication. (F) RHX was added at the time of initiation of replication, and cells were sampled 40 min later.

(G and H) Distances of the left (empty symbols, dashed lines) and right (filled symbols, solid lines) replication forks from *oriC* are plotted as a function of time after initiation of replication. Cells were synchronized for the replication cycle, and DNA content was determined as above. Where indicated, RHX, SHX, or norvaline was added 20 min (vertical arrows) after replication initiation. (G) Cells without (squares) and with (triangles) RHX are shown. The location of the proposed replication-arrest sites (Autret et al., 1999; Levine et al., 1991, 1995) is indicated (gray bar) on the y axis. (H) Cells without (squares) and with (triangles) SHX or norvaline (circles) are shown.

might otherwise occur with uncontrolled replication during starvation.

RESULTS

Monitoring Replication Elongation with DNA Microarrays

We used DNA microarrays to follow the progression of replication forks in *B. subtilis*, as has been done in *E. coli* (Khodursky et al., 2000). We synchronized a population of cells so that replication initiated at the same time in the majority of cells, and we measured the relative amount of DNA that corresponded to nearly all the genes at different times during replication (strains are listed in Table 1). Synchronization was achieved as described (Autret et al., 1999; Lemon and Grossman, 2000; Levine et al., 1991, 1995) using a temperature-sensitive mutant of a replication initiation protein (DnaB). Briefly, cells are incubated at the nonpermissive temperature to allow ongoing rounds of replication to finish. A new round of replication initiates after cells are shifted to permissive temperature. DNA samples were collected at various times, labeled with Cy5, mixed with Cy3-labeled reference DNA from cells with fully replicated chromosomes, and hybridized to DNA microarrays. The ratio of Cy5 to Cy3 represents the gene dosage and was determined for each gene spot and plotted versus gene position (Figures 1B–1F). Following replication, gene dosage doubled, and the average positions of the replication forks could be mapped and followed as the forks moved from *oriC* toward *ter* (Figures 1B–1E).

The average rate of replication was $\sim$0.45–0.55 kb/s at 30°C for both the left and right forks (Figures 1G and 1H). This rate is slower than that in *E. coli* at 30°C (0.61–0.75 kb/s; Breier et al., 2005; Khodursky et al., 2000). We noticed that one replication fork was slightly and consistently ahead of the other, which is similar to what was observed in *E. coli* (Breier et al., 2005).

Replication Arrests throughout the Chromosome upon Amino Acid Starvation

We observed that replication forks arrested near *oriC* if amino acid starvation was induced at the same time that replication initiated, which is consistent with previous reports (Autret et al., 1999; Levine et al., 1991, 1995). Addition of arginine hydroxamate (RHX), a nonfunctional arginine analog, quickly inhibited cell growth, causing the doubling time to increase from $\sim$55 min to >400 min. Forty minutes after replication initiation in cells treated with RHX, forks were $\sim$160 kb on either side of *oriC*

Table 1. *B. subtilis* Strains Used

Strains	Genotype
JH642 (AG174)	*trpC2 pheA1*
BB914	*ΔrelA::mls*[a]
JDW119	*Δrtp::kan*
JDW154	*dnaB134ts hutM⁺-lacO cat thrC::(Ppen-lacIΔ11-gfp(mut2) mls) polC::(polC-myc spc) Δrtp::kan*
JDW194	*dnaB134ts-zhb83::(Tn917 cat) Δrtp::kan*
JDW197	*dnaB134ts-zhb83::(Tn917 cat) ΔrelA::mls*
JDW278	*pHV1610 (cat)*[b]
JDW280	*pHV1610-1 (cat)*[b]
KPL69	*dnaB134ts-zhb83::(Tn917 mls)*
KPL151	*dnaB134ts-zhb83::(Tn917 cat)*
KPL382	*dnaX::(dnaX-gfp(mut2) spc)*[c]
KPL544	*hutM⁺-lacO cat thrC::(Ppen-lacIΔ11-gfp(mut2) mls)*[c]
KPL549	*dnaB134ts hutM⁺-lacO cat thrC::(Ppen-lacIΔ11-gfp(mut2) mls) polC-myc spc*[c]
LAS40	*PY79 recA::(recA-gfp spc)*[d]

[a] Wendrich and Marahiel, 1997.
[b] Bruand et al., 1995.
[c] Lemon and Grossman, 2000.
[d] Simmons et al., 2007.

(Figure 1F). In untreated cells, replication forks were much further along the chromosome, ~500–700 kb to either side of *oriC* (Figure 1D).

This observation appeared to support the model that *cis*-acting sites (LSTer and RSTer) ~100–200 kb to each side of *oriC* mediate a starvation-induced replication arrest (Autret et al., 1999). However, this model predicts that if replication forks already passed the putative *oriC*-proximal arrest sites, then their progression should not be inhibited by starvation.

To test this prediction, we induced starvation by adding RHX 20 min after initiation of replication, when forks have already proceeded ~400–500 kb from *oriC* and passed the proposed arrest sites in the ~100–200 kb region (Figures 1G and 2A). We found that replication forks still arrested within 10 min after amino acid starvation (Figure 1G) ~600–700 kb from *oriC* (Figure 2B), which demonstrates that starvation-induced replication arrest can take place not just near *oriC*, but elsewhere on the chromosome.

Our results indicate that replication might arrest throughout the chromosome soon after starvation. Alternatively, there may be additional arrest sites on the chromosome ~600–700 kb from *oriC*. We distinguished between these possibilities by evaluating the effects of starvation on asynchronous cell replication, in which replication forks could be anywhere on the chromosome. We
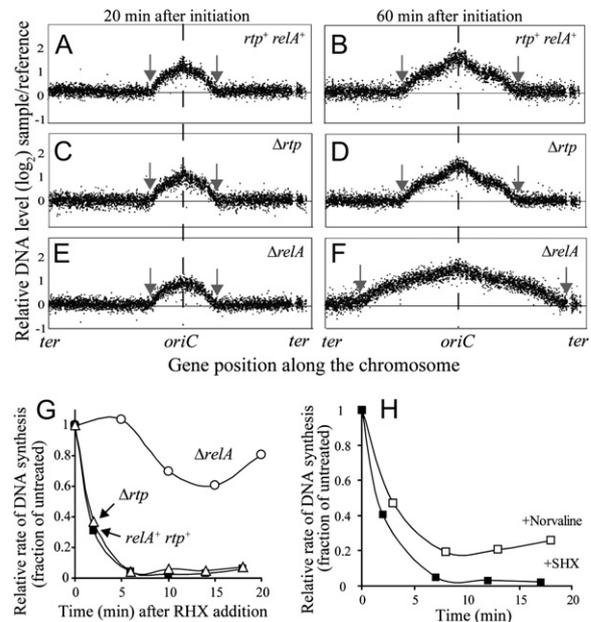

Figure 2. Replication Arrest Induced by Amino Acid Starvation Depends on *relA* but Not *rtp*

(A–F) Cells were synchronized for the replication cycle, and DNA content was analyzed as in Figure 1. RHX was added 20 min after replication initiation. Samples were taken 20 min after replication initiation (immediately before addition of RHX; panels A, C, and E) and 60 min after replication initiation (40 min after addition of RHX; panels B, D, and F). Arrows indicate positions of replication forks. (A) and (B) show *rtp⁺ relA⁺* cells (KPL151); (C) and (D) show *Δrtp* (JDW163); and (E) and (F) show *ΔrelA* (JDW184).

(G and H) Effects of amino acid starvation on asynchronous replication are shown. Cells were grown to midexponential phase (OD_600 ~0.3) at 37°C. The relative rate of DNA synthesis (incorporation of ³H-thy into DNA of treated samples normalized to untreated) is plotted as a function of time after amino acid starvation. (G) Relative rate of DNA synthesis after treatment with RHX is shown. Filled squares indicate *relA⁺ rtp⁺* (JH642); open triangles indicate *Δrtp* (JDW119); and open circles indicate *ΔrelA* (BB914). (H) shows relative rate of DNA synthesis in wild-type (JH642) after treatment with SHX (filled squares) or norvaline (open squares).

observed virtually complete inhibition of replication shortly after amino acid starvation. The rate of replication was measured by pulse labeling with ³H-thymidine (³H-thy) and by measuring the incorporation of ³H-thy into the trichloroacetic acid (TCA)-precipitable fractions. At 30°C, incorporation of ³H-thy was reduced ~50% in ~2–4 min and was at background levels (≤200 cpm in a 2 min pulse) within ~10 min after addition of RHX. In the absence of RHX, there were >16,000 cpm per optical density (OD) unit of cells incorporated in a 2 min pulse. At 37°C, incorporation was reduced to ~50% in ~1–2 min and was at background levels within ~6 min (Figure 2G).

The inhibition of ³H-thy incorporation by starvation was not due to inhibition of thymidine uptake. We measured uptake of ³H-thy and found no significant effect after treatment of cells with RHX (data not shown). Taken together, these results demonstrate that replication arrests shortly

after amino acid starvation, irrespective of the location of the replication forks.

Starvation-Induced Replication Arrest Does Not Depend on Rtp

In *B. subtilis*, replication is normally arrested at *ter* sites by Rtp (Duggin and Wake, 2002). It was proposed that Rtp also mediates replication arrest upon amino acid starvation (Levine et al., 1995). To investigate the role of Rtp in mediating replication arrest in response to starvation, we monitored fork progression in a strain lacking Rtp (Δ*rtp*). Replication forks were in approximately the same location in *rtp*[+] and Δ*rtp* cells before addition of RHX (Figures 2A and 2C). After induction of amino acid starvation with RHX, we found that replication forks arrested in the same regions of the chromosome in *rtp*[+] and Δ*rtp* cells (Figures 2B and 2D), indicating that starvation-induced replication arrest does not depend on Rtp.

We also monitored the rate of asynchronous replication in *rtp* mutant cells using ^{3}H-thy incorporation. We found that the addition of RHX caused replication arrest to a similar extent in Δ*rtp* and *rtp*^{+} cells (Figure 2G).

Previous work showed that starvation-induced replication arrest near *oriC* can be observed by determining the copy number of *oriC*-proximal genes using fluorescence microscopy (Dworkin and Losick, 2002; Lemon and Grossman, 2000). Using essentially the same method (Lemon and Grossman, 2000), we observed that Rtp was not required for starvation-induced replication arrest near the proposed LSTer site (Supplemental Data).

Taken together, these results show that starvation-induced replication arrest occurs throughout the chromosome and does not require Rtp, the protein that is normally involved in arresting replication forks at the *ter* sites.

Starvation-Induced Replication Arrest Requires the Stringent Response

RelA, the enzyme essential for the stringent response (Cashel et al., 1996; Wendrich and Marahiel, 1997), was previously found to be required for starvation-induced replication arrest near *oriC* (Levine et al., 1991). We found that RelA is required for starvation-induced replication arrest throughout the chromosome. We monitored replication-fork progression using DNA microarrays in a Δ*relA* mutant that had been synchronized for the replication cycle (Figures 2E and 2F). We also monitored the rate of replication in asynchronous cultures using ^{3}H-thy incorporation (Figure 2G). In both experiments, we found that the *relA* mutant did not arrest replication after addition of RHX. These results demonstrate that the starvation-induced replication arrest that occurs throughout the chromosome is mediated by the stringent response.

Starvation-Induced Replication Arrest Is Not Mediated by the Effects of the Stringent Response on Transcription

The best characterized effects of the stringent response are global transcription changes, especially decreased transcription of rRNA and tRNA operons (Cashel et al., 1996). Using microarrays to monitor changes in mRNA levels in response to RHX treatment, we observed that transcription of many genes decreased while transcription of some genes increased (data not shown), which is similar to previous work (Eymann et al., 2002).

To test whether replication arrest was mediated by decreased transcription, we inhibited transcription by adding rifampicin and monitored replication forks. Treatment of cells with rifampicin resulted in rapid inhibition of transcription (Figure 3A). Replication-fork progression, as monitored by microarrays, was not affected (data not shown). Furthermore, we observed that rifampicin treatment increased incorporation of ^{3}H-thy into DNA by increasing the uptake of thymidine into the cells (Figures 3B and 3C).

To test whether the stringent response mediates replication arrest by increasing transcription of some genes, we examined whether replication can still be inhibited by starvation in the absence of de novo transcription. RHX was added 1.5 min after rifampicin, when transcription was severely inhibited (Figure 3A). Replication was still rapidly arrested upon addition of RHX (Figure 3B) despite the inhibition of transcription. These results indicate that the starvation-induced replication arrest is not a consequence of RelA-mediated changes in transcription.

Replication Elongation Is Inhibited by Increased (p)ppGpp Rather Than Decreased GTP

Upon amino acid starvation, RelA synthesizes the small nucleotides (p)ppGpp from ATP and GTP. We observed that ppGpp (Figure 3D) and pppGpp (not shown) accumulated immediately after RHX addition and reached a plateau within 10 min. The increase in (p)ppGpp was accompanied by a decrease in GTP (Figure 3E), most likely due to the use of GTP to synthesize (p)ppGpp and the inhibition of IMP dehydrogenase, the first enzyme in GTP biosynthesis, by (p)ppGpp (Lopez et al., 1981). Intracellular ATP did not decrease (Figure 3F).

In *B. subtilis*, decreases in GTP levels mediate several of the RelA-dependent responses to starvation (Inaoka and Ochi, 2002; Krasny and Gourse, 2004; Ochi et al., 1982; Vasantha and Freese, 1980). To test if starvation-induced replication arrest is mediated by elevated levels of (p)ppGpp and/or by decreased levels of GTP, we uncoupled changes in GTP and (p)ppGpp using two approaches. First, we lowered GTP levels without affecting (p)ppGpp by treating cells with decoyinine, a selective inhibitor of the synthesis of GMP (a precursor of GTP), that has been used to differentiate the effects of GTP from those of (p)ppGpp (Lopez et al., 1981; Ochi et al., 1982; Vasantha and Freese, 1980). As expected, decoyinine treatment reduced GTP levels to 30%–40% of those in untreated cells within 4 min (Figure 3E) and reduced the growth rate (data not shown). The rate of replication in decoyinine-treated cells was nearly normal after 8 min and decreased only gradually afterwards (Figure 3B). These
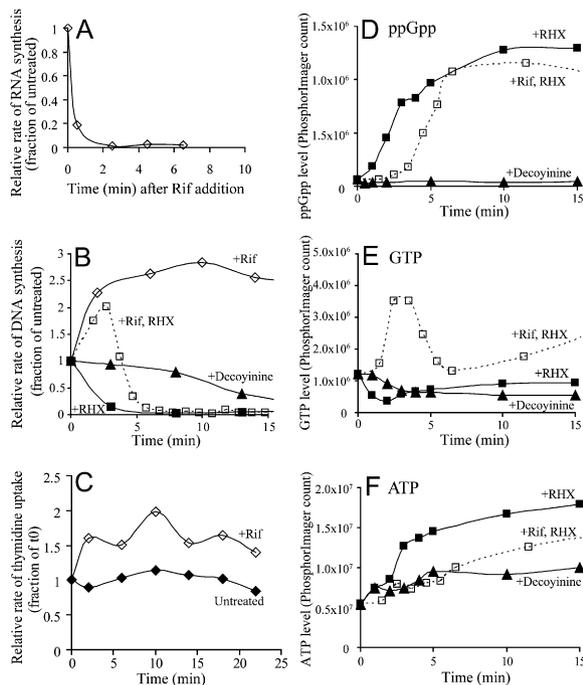
Figure 3. Starvation-Induced Replication Arrest Is Dependent on Accumulation of (p)ppGpp and Independent of Transcription

Wild-type cells (JH642) were grown at 37°C and treated as indicated. Rifampicin was added at t = 0 (open diamonds). RHX was added at t = 0 (filled squares). Rifampicin was added at t = 0, and RHX was added 1.5 min later (open squares and dotted lines). Decoyinine was added at t = 0 (filled triangles). Filled diamonds indicate untreated cells.
(A) Rifampicin rapidly inhibits transcription. The rate of transcription was measured by pulse labeling cells with ^{3}H-uridine for 1 min, measuring incorporation of ^{3}H-uridine into TCA-precipitable fractions, and normalizing to an untreated sample. The normalized rate is plotted as a function of time after addition of rifampicin.
(B) Rates of replication are shown. The rate of replication was measured as described (Figures 2G and 2H) and is plotted as a function of time after the indicated treatment.
(C) Addition of rifampicin increases uptake of ^{3}H-thy into cells. The rate of uptake was obtained by pulse labeling cells with ^{3}H-thy for 2 min, measuring ^{3}H-thy retained in cells, normalizing to cells at t = 0, and plotting the normalized rate as a function of time after indicated treatment.
(D–F) Effects of indicated treatments on levels of ppGpp (D), GTP (E), and ATP (F) are shown. Cultures were labeled with ^{32}P-inorganic phosphate, and nucleotides were extracted, separated by TLC, and quantified using a PhosphorImager. The total PhosporImager count for each spot is plotted as a function of time after the indicated treatment. Results from one experiment are shown and are representative of ≥2 experiments. Not shown: pppGpp accumulated with similar kinetics as ppGpp, but pppGpp levels were ∼4-fold higher than those of ppGpp.

results indicate that decreasing the level of GTP does not directly lead to replication arrest.

We also observed that starvation-induced replication arrest occurs when (p)ppGpp increase without a significant decrease in GTP. To elevate (p)ppGpp levels without causing a significant drop in GTP, we inhibited transcrip-

tion with rifampicin before inducing starvation. Inhibition of transcription reduces GTP consumption, causing a significant increase in GTP (data not shown). Addition of RHX 1.5 min after addition of rifampicin caused significant accumulation of (p)ppGpp, yet the GTP level remained >80% of that before treatment (Figures 3D and 3E). Replication was still quickly inhibited by RHX in the presence of rifampicin (Figure 3B) even though GTP was much higher than in cells treated with decoyinine or RHX alone (Figure 3E). Together, these results provide evidence that replication arrest is not caused by a decrease in GTP and indicate that the likely signals for the replication arrest are (p)ppGpp.

(p)ppGpp Directly Inhibit Primase

The rapid arrest of replication elongation following starvation appears to be mediated by (p)ppGpp. We tested potential targets of (p)ppGpp in vitro by measuring the effects of (p)ppGpp on the activities of purified components of the *B. subtilis* replication machinery. Addition of GDP, ppGpp, or pppGpp had little or no effect on the activity of the purified DNA polymerase catalytic subunit PolC (Figure 4A).

However, ppGpp and pppGpp, but not GDP, clearly inhibited the activity of purified primase (DnaG); pppGpp was a more potent inhibitor than was ppGpp (Figure 4B). The primase activity is not due to contamination of the protein preparations with RNA polymerase (RNAP), as rifampicin did not inhibit the activity (Figure 4B). The products synthesized in the primase assay could be extended by Klenow polymerase (Supplemental Data), indicating that they are bona fide primers. In addition, we found that ppGpp inhibits helicase-dependent primosome activity in vitro (G.M.S., unpublished data).

There was a good correlation between the concentrations of pppGpp and ppGpp (∼0.5–1 mM) that strongly inhibited primase in vitro and the estimated physiological concentrations of (p)ppGpp upon starvation. Our data indicate that the total concentration of pppGpp and ppGpp in vivo, after addition of RHX, is similar to the concentration of ATP, which is estimated to be 1–5 mM.

To test whether primase could be a target of (p)ppGpp in vivo, we used a plasmid (pHV1610-1) that contains a conditional and nonessential mechanism for lagging-strand synthesis (Bruand et al., 1995). pHV1610-1 replicates, in part, by the rolling-circle mechanism, and the presence of a primosome-assembly site allows lagging-strand synthesis. Upon inhibition of primase or primosome activity, lagging-strand synthesis is inhibited, but leading-strand synthesis continues, resulting in an increase in the amount of pHV1610-1 ssDNA in vivo (Bruand et al., 1995).

We found that addition of RHX caused a 2-fold increase in pHV1610-1 ssDNA in vivo (Figure 4C), indicating that amino acid starvation likely inhibits the primosome. As a control, no increase in ssDNA was observed after similar starvation of cells containing the plasmid pHV1610 (data not shown). pHV1610 is the same as pHV1610-1 except that it lacks the site required for primosome-dependent
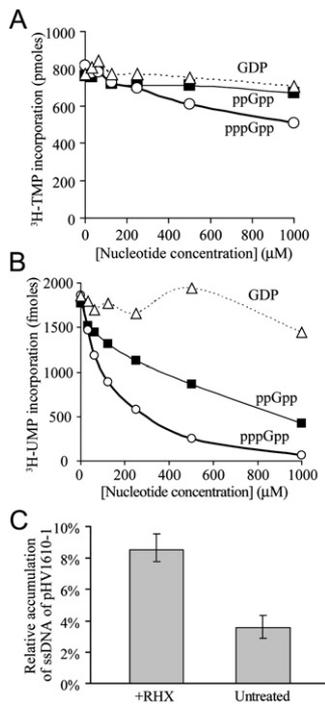
Figure 4. Effects of (p)ppGpp and Amino Acid Starvation on DNA Polymerase and Primase Activity

(A and B) Activity of purified *B. subtilis* DNA polymerase PolC (A) or primase DnaG (B) in vitro is shown. PolC gap-filling activity (A) or primase activity (B) is plotted as a function of indicated concentrations of GDP (open triangles), ppGpp (filled squares), and pppGpp (open circles). Primase activity in the presence of 25 μg/ml of rifampicin is shown. Primase activity in the absence of rifampicin is similar (data not shown). (C) shows increase in plasmid ssDNA upon treatment with RHX. DNA was purified from cells containing plasmid pHV1610-1 (JDW280). Plasmid ssDNA and dsDNA forms were separated on agarose gels, transferred to nylon membranes, and hybridized with a labeled plasmid probe. The percentage of ssDNA relative to the covalently closed circular dsDNA of pHV1610-1 was determined for cells left untreated or treated with RHX for 20 min. Inhibition of primase is known to cause an ∼2-fold increase in pHV1610-1 ssDNA (Bruand et al., 1995).

lagging-strand synthesis and is not affected by inhibition of primase or the primosome (Bruand et al., 1995).

Together, the in vivo and in vitro results strongly indicate that primase, an essential component of the primosome, is inhibited by the starvation-signaling nucleotides (p)ppGpp.

Replication Elongation Is Inhibited by (p)ppGpp in a Dose-Dependent Manner In Vivo

The in vitro results indicate that there is a dose-dependent relationship between the concentrations of (p)ppGpp and inhibition of primase (Figure 4B). A dose-dependent relationship in vivo could indicate a tunable form of control of replication elongation. Addition of RHX to cells severely inhibits replication (Figures 1G and 2G), perhaps because (p)ppGpp levels reach higher concentrations than what are required for inhibiting primase activity in vitro

(K_i ∼0.25–0.5 mM for ppGpp and 0.12 mM for pppGpp). Similarly, addition of serine hydroxamate (SHX), another strong inducer of (p)ppGpp, caused severe inhibition of replication (Figures 1H and 2H).

In contrast, addition of norvaline (starvation for isoleucine and leucine), which results in (p)ppGpp accumulation to ∼25% of that caused by SHX (Belitskii and Shakulov, 1980), caused a partial inhibition of cell growth; the doubling time increased from ∼55 min to ∼125 min. Norvaline caused a drop in the rate of replication to 20%–25% of that in untreated cells, as measured by incorporation of ^{3}H-thy (Figure 2H). The partial inhibition of replication was due to a decreased average rate of elongation in the population of cells as measured using DNA microarrays (Figure 1H). We conclude that high levels of (p)ppGpp induce replication arrest and that lower levels of (p)ppGpp slow the rate of replication.

(p)ppGpp-Arrested Replication Forks Do Not Appear to Recruit RecA

In addition to the stringent response, various other situations can cause replication-fork arrest. These situations include exhaustion of dNTPs, DNA damage, and collisions with replication roadblocks, e.g., stalled transcription complexes (Foti et al., 2005; Michel et al., 2004; Trautinger et al., 2005). The recombination protein RecA is recruited to ssDNA at arrested forks (reviewed in Courcelle and Hanawalt, 2003; Lusetti and Cox, 2002; Michel et al., 2004).

To investigate the state of the replication forks during starvation-induced arrest, we examined whether the arrested forks recruit RecA. We visualized functional RecA-GFP expressed from the endogenous promoter (Simmons et al., 2007) in living cells. In most untreated cells, RecA-GFP fluorescence filled the cells without discernable foci. A minority of untreated cells (14%) contained RecA-GFP foci or filaments (Figure 5A), indicating a low level of replication-fork disruption that leads to the recruitment of RecA during normal growth, similar to that observed previously (Renzette et al., 2005; Simmons et al., 2007). For simplicity, we use "foci" to describe both foci and filaments. When cells were treated with 6-(p-hydroxyphenylazo)-uracil (HPUra), an inhibitor of DNA polymerase (Brown, 1970), foci of RecA-GFP formed in 97% of the cells (Figures 5B and 5E). Similarly, depletion of dNTP pools by addition of hydroxyurea (HU), an inhibitor of dNTP synthesis (Timson, 1975), led to formation of RecA-GFP foci in 87% of the cells (Figures 5C and 5E).

In contrast, addition of RHX did not stimulate formation of RecA-GFP foci; only 16% of cells treated with RHX had foci (Figures 5D and 5E). Therefore, arrest of replication forks by (p)ppGpp does not appear to recruit RecA.

Replication arrest induced by amino acid starvation is reversed upon addition of excess nutrients (Copeland, 1971; Dworkin and Losick, 2002; Lemon and Grossman, 2000; Levine et al., 1991). We found that (p)ppGpp-arrested replication forks restart without RecA. Treatment of a *recA* null mutant with RHX for 40 min at 37°C did not lead to loss of cell viability, as judged by the ability
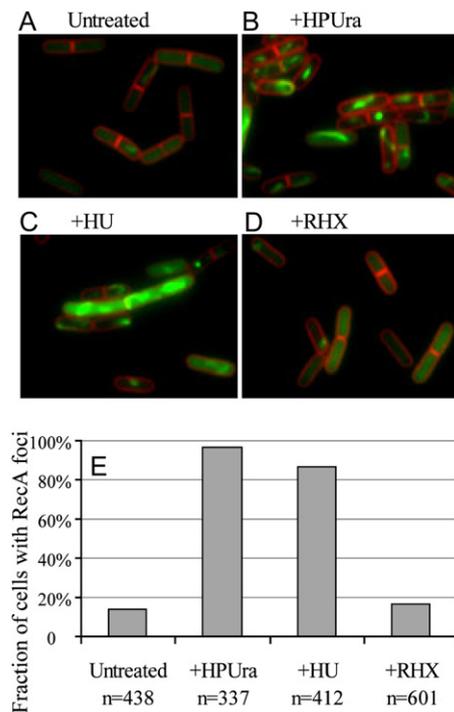
Figure 5. Arrest of Replication by Amino Acid Starvation Does Not Induce Formation of RecA-GFP Foci

Focus formation was monitored by fluorescence microscopy. Cells with a functional *recA-gfp* fusion (LAS40) were grown at 30°C and treated as indicated for 40 min before observation.

(A–D) Micrographs of cells containing RecA-GFP (green diffuse background or foci) with membranes stained with FM4-64 (red) are shown. Cells were left untreated (A); treated with HPUra (38 μg/ml; B), which binds to and inhibits DNA polymerase; treated with hydroxyurea (4 mg/ml; C), which depletes dNTP pools; or treated with RHX (D).

(E) Fractions of cells with discernable RecA-GFP foci and the treatments and total number of cells measured (n) are indicated.

of cells to form colonies after removal of RHX (data not shown). These results indicate that amino acid starvation induces replication arrest and that forks remain competent to resume replication, once nutrients become available, without activation of a RecA-dependent recombination pathway.

DISCUSSION

We characterized a mechanism for regulating replication elongation in response to a sudden shift in nutrient availability in *B. subtilis*. We found that progression of replication forks, regardless of their positions along the chromosome, stops within minutes of induction of the stringent response by amino acid starvation. This arrest is mediated by small nucleotides (p)ppGpp, likely by direct inhibition of the essential replication component primase. High levels of (p)ppGpp stop replication, and lower levels slow replication. The (p)ppGpp-mediated arrest differs from replication arrest caused by DNA damage or dNTP depletion in

that it does not appear to recruit RecA. Our results indicate that (p)ppGpp directly mediate the rapid, stable, reversible, and tunable control of replication elongation in response to nutritional status.

When cells are starved at the time of replication initiation, replication forks arrest near the proposed STer sites proximal to *oriC*, and this was proposed to be mediated by Rtp (Autret et al., 1999; Levine et al., 1991, 1995). We believe that there appeared to be *oriC*-proximal arrest sites due to the specific timing of starvation in these experiments. Our results indicate that the arrest can occur throughout the chromosome and are consistent with an earlier study that found that replication stops throughout the chromosome after amino acid starvation of asynchronous cultures (Copeland, 1971). We also found that Rtp is not required for replication arrest induced by the stringent response. Rtp-binding sites have been found in the LSTer region and mediate replication arrest on a plasmid (Autret et al., 1999), but this arrest is independent of the stringent response (Gautam and Bastia, 2001) and is probably not related to the *rtp*-independent arrest described here.

Primase Appears to Be a Target for Control of Replication by (p)ppGpp

In vitro and in vivo results indicate that primase is a likely target of (p)ppGpp. (p)ppGpp couple the cellular metabolic state to transcription and translation by targeting RNAP and, perhaps, the translation initiation factor IF-2 (Cashel et al., 1996; Milon et al., 2006). Primase synthesizes RNA using DNA as template, analogous to RNAP. Molecular characterization of the (p)ppGpp-primase interaction should provide mechanistic insights into how ppGpp inhibits primase.

Primase activity is required for lagging-strand synthesis, which, for replication of the chromosome, is normally coupled to leading-strand synthesis (Pages and Fuchs, 2003). Inhibition of primase should cause a decrease in both lagging- and leading-strand synthesis of chromosomal DNA. In addition, binding of (p)ppGpp to primase might result in allosteric inhibition of other components of the replication complex through protein-protein interactions. Primase and the replicative helicase interact directly and regulate each other's activity (reviewed in Baker and Bell, 1998; Corn and Berger, 2006; Soultanas, 2005). Inhibition of primase activity might inhibit helicase activity through direct interaction.

Primase seems to be a natural entry point for control of replication elongation. It is required continuously during elongation, as each Okazaki fragment requires an RNA primer. During T7-phage DNA replication, primase temporarily pauses replication during primer synthesis (Lee et al., 2006). In addition, eukaryotic primase activity is essential for checkpoint pathways that couple replication to mitosis (Griffiths et al., 2001; Michael et al., 2000). Together with our work, these results highlight the importance of primase in coordinating replication with other cellular events.

Role of (p)ppGpp-Mediated Replication Arrest in Genomic Stability

Many circumstances cause replication arrest, including dNTP depletion, DNA damage, and other roadblocks. In these circumstances, the arrested forks recruit RecA to the site of arrest (Foti et al., 2005; Michel et al., 2004; Trautinger et al., 2005). RecA is important for recombination, repair, and induction of the SOS response (Courcelle and Hanawalt, 2003; Lusetti and Cox, 2002; Walker, 1996). We found that (p)ppGpp-arrested replication forks do not recruit RecA, which indicates that the recombination pathway is not strongly activated during (p)ppGpp-mediated replication arrest.

How might (p)ppGpp-mediated replication arrest differ from other arrests that activate the recombination pathway? One possibility is that (p)ppGpp-arrested replication forks lack the extensive regions of ssDNA that recruit RecA. Inhibition of primase by (p)ppGpp might halt the replicative helicase, causing arrest of replication without generating large regions of ssDNA. Alternatively, there might be mechanisms that prevent recombination pathways from being activated at (p)ppGpp-arrested forks and perhaps checkpoint proteins that stabilize forks arrested by inhibition of primase. In *E. coli,* the GTP-binding protein Obg can stabilize arrested replication forks (Foti et al., 2005).

We propose that the rapid and reversible replication arrest mediated by (p)ppGpp helps maintain genomic stability by preventing deleterious consequences associated with replication in starving cells. Starvation presents potential challenges to replication, e.g., by causing an eventual depletion of essential substrates. Starvation could lead to a rapid decrease in dNTPs. The dNTP pools are sufficient to support replication for <1 min (Werner, 1971) and need constant replenishment. Continued replication upon depletion of dNTPs can cause double-strand breaks, and rescue of these breaks often results in mutagenesis and recombination; failure to rescue leads to cell death (Michel et al., 2004). Regulation of replication initiation might not be sufficient to respond to the challenge of starvation. Once initiated, replication of the *B. subtilis* chromosome takes ~50 min. In contrast, arrest of elongation mediated by (p)ppGpp occurs within 5–10 min of starvation. Under these conditions, the replication forks are less likely to be subjected to the danger of being disrupted by dNTP depletion or other adverse conditions. After nutrients are available again, the arrested forks can resume replication with minimum disturbance to the genome.

It will be interesting to characterize the long-term effects of (p)ppGpp on replication. The stringent response is crucial during transient nutrient stress, when the balance between nutrient availability and cellular activity is altered. Once a balance is restored, (p)ppGpp levels drop (Cashel et al., 1996). If cells are subjected to prolonged starvation and replication arrest, restart of replication might utilize specialized proteins involved in stress-induced mutagenesis (Sung and Yasbin, 2002). Under these circumstances, the (p)ppGpp-mediated arrest that prevents genomic in-

stability during transient nutrient stress might be involved in generating genomic variation.

Mechanisms that modulate replication elongation and prevent replication-fork disruption might be more widespread than previously recognized. During some developmental stages in *Tetrahymena* and *Xenopus*, replication elongation arrests or pauses at replication-fork barriers or pause sites in rDNA (Maric et al., 1999; Zhang et al., 1997). Yeasts are able to arrest replication elongation before dNTP pools are exhausted (Koc et al., 2004), and *B. subtilis* uses (p)ppGpp to directly regulate the replication machinery. Direct regulation of replication elongation may constitute part of the complex regulatory mechanisms that protect organisms from genomic instability.

EXPERIMENTAL PROCEDURES

Strains, Media, and Growth

Standard procedures were used for genetic manipulations (Harwood and Cutting, 1990). All *B. subtilis* strains (Table 1) are derived from JH642, except LAS40 (which was derived from the prototroph PY79). Amino acid starvation was induced by addition of RHX (0.5 mg/ml), SHX (1.5 mg/ml), or norvaline (0.5 mg/ml). Decoyinine (0.5 mg/ml) was used to reduce GTP without causing a significant increase in (p)ppGpp. Rifampicin (1 mg/ml) was added to inhibit transcription.

For all experiments presented, cells were grown with shaking at 30°C or 37°C in defined minimal medium (Vasantha and Freese, 1980) with MOPS buffer at 50 rather than 100 mM, then supplemented with 0.1% glutamate, 1% glucose, and required amino acids. For measurement of nucleotide levels, phosphate was reduced from 5 to 0.5 mM.

Replication cycles in a population of cells were synchronized using the temperature-sensitive replication initiation mutant *dnaB134ts* that fails to initiate new rounds of replication at the nonpermissive temperature 45°C, as described in the text.

Use of Genomic Microarrays to Study DNA Replication

DNA microarrays contained PCR products from >99% of the annotated *B. subtilis* open reading frames spotted onto Corning GAPS II slides, as described (Britton et al., 2002). Cells were collected and mixed with an equal volume of ice-cold methanol. Chromosomal DNA was extracted and purified on columns from the Qiagen genomic DNA kit, fragmented by digesting with HaeIII, and purified on Qiagen QiaQuick PCR purification columns. 0.5 μg of DNA was incubated with 7.5 μg random hexamers at 95°C for 5 min, rapidly cooled on ice, then incubated with 20 units of Klenow exo- (NEB) and a dNTP mixture (0.1 mM dTTP, 0.5 mM dATP, 0.5 mM dGTP, 0.5 mM dCTP, and 0.4 mM aminoallyl-dUTP [Ambion]) at 30°C overnight. DNA labeled with aminoallyl-dUTP was purified on Qiagen MinElute columns. 50 mM NaHCO$_3$ (pH 9.0) and the fluorescent dye Cy5 or Cy3 (Amersham) were added, and the dye-coupling reaction was incubated for 1 hr at room temperature in the dark. The labeling was quenched with 1.2 M hydroxylamine for 15 min. The Cy5-labeled genomic DNA sample was mixed with Cy3-labeled reference DNA, purified on MinElute columns, and hybridized to microarrays.

Thymidine/Uridine Incorporation/Uptake

Cells were grown to midexponential phase, and 0.2 ml of culture was pulse labeled with 10 μl of ^{3}H-uridine (40 Ci/mmol; 1 mCi/ml) or ^{3}H-thy (80 Ci/mmol; 1 mCi/ml) for 1 or 2 min.

To measure RNA or DNA synthesis (incorporation of radioactive label into nucleic acid), ice-cold TCA (final concentration 10%) was mixed with labeled samples and incubated on ice for ≥30 min. Samples were filtered on glass-fiber filters (GF6, Schleicher & Schuell) with vacuum and washed three times with 10 ml of ice-cold 5% TCA. Filters

were dried, added to scintillation fluid, and the amount of radioactivity that had been incorporated into nucleic acid was determined by scintillation counting.

To measure uptake of radioactive label into cells, samples (not treated with TCA) were filtered onto 0.45 μ membrane filters (Pall Life Sciences Metricel GN-6) and washed multiple times with 0.1 M LiCl. The amount of radioactivity remaining in the cells on the filter was determined by liquid scintillation counting.

Measurement of Intracellular Nucleotides

Previously published protocols were used with minor modifications (Schneider et al., 2003). Cultures were started at $OD_{600} \leq 0.001$. At $OD_{600} \sim 0.05$, $KH_2{}^{32}PO_4$ (1 Ci/mmol; 1 mCi/ml; Perkin Elmer) was added to a final concentration of 50 μCi/ml. At $OD_{600} \sim 0.6$, 0.2 ml of culture was mixed with 0.04 ml 2 M ice-cold formic acid, left on ice for ≥ 20 min, and centrifuged at 4°C for ≥ 15 min to collect the supernatant. TLC plates were prepared and loaded as described (Schneider et al., 2003). For optimal separation of ppGpp and pppGpp, plates were developed in 1.5 M KH_2PO_4 (pH = 3.4). For optimal separation of GTP, plates were developed in 0.85M KH_2PO_4. Plates were exposed to a Storage Phosphor Screen and quantified using a Molecular Dynamics Typhoon scanner.

Microscopy

Cells were sampled during exponential growth. The vital membrane dye FM4-64 was added (0.05 μg/ml) 10 min before sampling. DAPI (4,6-diamidino-2-phenylindole) was added (0.1 μg/ml) before cells were placed on pads of 1% agarose in minimum salts with 1 mM $MgSO_4$. Fluorescence was viewed with a Nikon E800 microscope equipped with a ×100 differential interference contrast objective and appropriate filters. Images were obtained with a cooled charge-coupled device camera (model C4742-95; Hamamatsu) and were analyzed using Improvision OpenLab software.

Purification and Overexpression of Hexahistidine-Tagged *B. subtilis* Primase

B. subtilis dnaG (primase) was cloned into a pET28-derived vector and overexpressed by standard methods. Cell paste (50% w/v in 50 mM Tris [pH 8.0], 10% v/v sucrose) was thawed, and 1 volume of buffer (80 mM Hepes [pH 7.8], 20% v/v glycerol, 800 mM NaCl, 20 mM imidazole, and 10 mM β-mercaptoethanol) and Brij 58 (to 0.5%) were added. The mixture was sonicated, and debris was removed by centrifugation. The crude extract was loaded onto a nickel-NTA column and washed with 10 column volumes of buffer (40 mM Hepes [pH 7.8], 750 mM NaCl, 20 mM imidazole, 10% glycerol, and 5 mM β-mercaptoethanol). Proteins were eluted in the same buffer plus 150 mM imidazole. Primase-containing fractions were dialyzed (40 mM Hepes [pH 7.8], 50 mM NaCl, 0.1 mM EDTA, 1 mM dithiothreitol, 10% v/v glycerol) and loaded onto a Q-Sepharose column equilibrated in the same buffer. The column was washed with 5 column volumes of this buffer. Proteins were eluted with a gradient to 0.5 M NaCl over 10 column volumes. Primase was eluted at ∼0.3 M NaCl. Fractions were analyzed by SDS-PAGE and pooled, then glycerol was added to 20% v/v, and the fractions were aliquotted, frozen in liquid nitrogen, and stored at −80°C. Primase activity was stable for at least one year.

Scintillation Proximity Assay of *B. subtilis* Primase Activity

Reactions (25 μl) contained 36 mM Hepes-NaOH (pH 7.5); 10 mM MgOAc; 4% glycerol 0.0127% w/v NP40; 20 μM TCEP; 8.8 nM single-stranded M13 DNA (MP18); 30 μM ATP, GTP, and CTP; 0.286 μM ^{3}H-UTP (specific activity 35 Ci/mmol); 100 nM primase; and the indicated amount of ppGpp (Trilink Inc), pppGpp (a gift from M. Cashel), or GDP in microtiter plates. Reactions were incubated at 37°C for 1 hr and stopped with EDTA (50 mM). One hundred micrograms polyethyleneimine-polyvinyltoluene scintillation proximity assay (SPA) beads (Amersham, PEI-PVT SPA beads) in 0.3 M sodium citrate (pH 3.0) were added, and the mix was incubated for 30 min at room temperature. The plates were centrifuged at 1000 g for 7 min, and radioactivity associated with the beads was measured by scintillation counting.

SPA of Gap-Filling Activity of *B. subtilis* PolC

B. subtilis PolC was purified as described (Barnes and Brown, 1995). Reactions (25 μl) contained 36 mM Hepes-NaOH (pH 7.5); 10 mM MgOAc; 4% glycerol 0.02% w/v Pluronic F68; 0.2 μg/ml gapped (DNase I-treated) calf thymus DNA; 48 μM ATP, GTP, and CTP; 18 μM ^{3}H-dTTP (18 Ci/mmol); 18 nM PolC; and the indicated amount of ppGpp, pppGpp, or GDP in microtiter plates. Reactions were incubated at 37°C for 15 min and stopped with EDTA (50 mM). SPA beads were added and samples processed as described for the primase assay.

Measurement of Plasmid ssDNA and dsDNA

We used Southern blots to measure the amounts of plasmid ssDNA and dsDNA in vivo (Bruand et al., 1995). ssDNA was detected on blots from both native and denatured gels. dsDNA was detected only on blots from denatured gels. Cells containing pHV1610-1 or pHV1610 were grown to midexponential phase in minimal medium at 37°C. Cells (0.7 ml) were added to 0.7 ml of ice-cold methanol and harvested by centrifugation. DNA was purified by a neutral lysis method and treated with RNase (Harwood and Cutting, 1990). DNA samples were run in two 0.8% agarose gels with ethidium bromide (0.5 μg/ml). One gel was denatured in 1.5 M NaCl and 0.5 M NaOH for 25 min followed by neutralization in 1.5 M NaCl, 0.5 M Tris.HCl (pH 7.5) for 30 min. DNA from both the denatured and native gels was transferred to GeneScreen nylon membranes (Perkin Elmer), crosslinked, and hybridized to ^{32}P-labeled probes. Probes were made by random priming from a 1 kb PCR product from a region common to pHV1610-1 and pHV1610 using Megaprime DNA labeling (Amersham). Hybridization was at 65°C overnight. Membranes were washed, exposed on a Storage Phosphor Screen, and quantified using a Typhoon scanner.

Supplemental Data

Supplemental Data include Two Figures, Supplemental Results, and Supplemental References and can be found with this article online at http://www.cell.com/cgi/content/full/128/5/865/DC1/.

REFERENCES

Autret, S., Levine, A., Vannier, F., Fujita, Y., and Seror, S.J. (1999). The replication checkpoint control in Bacillus subtilis: identification of a novel RTP-binding sequence essential for the replication fork arrest after induction of the stringent response. Mol. Microbiol. *31*, 1665–1679.

Baker, T.A., and Bell, S.P. (1998). Polymerases and the replisome: machines within machines. Cell *92*, 295–305.

Barnes, M.H., and Brown, N.C. (1995). Purification of DNA polymerase III of gram-positive bacteria. Methods Enzymol. *262*, 35–42.

Belitskii, B.R., and Shakulov, R.S. (1980). Mol. Biol. (Mosk.) *14*, 1342–1353.

Breier, A.M., Weier, H.U., and Cozzarelli, N.R. (2005). Independence of replisomes in Escherichia coli chromosomal replication. Proc. Natl. Acad. Sci. USA *102*, 3942–3947.

Britton, R.A., Eichenberger, P., Gonzalez-Pastor, J.E., Fawcett, P., Monson, R., Losick, R., and Grossman, A.D. (2002). Genome-wide analysis of the stationary-phase sigma factor (sigma-H) regulon of Bacillus subtilis. J. Bacteriol. *184*, 4881–4890.

Brown, N.C. (1970). 6-(p-hydroxyphenylazo)-uracil: a selective inhibitor of host DNA replication in phage-infected Bacillus subtilis. Proc. Natl. Acad. Sci. USA *67*, 1454–1461.

Bruand, C., Ehrlich, S.D., and Janniere, L. (1995). Primosome assembly site in Bacillus subtilis. EMBO J. *14*, 2642–2650.

Cashel, M., Gentry, D.R., Hernandez, V.H., and Vinella, D. (1996). The stringent response. In Escherichia coli and Salmonella: Cellular and Molecular Biology, F.C. Neidhardt, R. Curtiss, III, J.L. Ingraham, E.C.C. Lin, K.B. Low, B. Magasanik, W.S. Reznikoff, M. Riley, M. Schaechter, and H.E. Umbarger, eds. (Washington, D.C.: ASM Press), pp. 1458–1496.

Copeland, J.C. (1971). Regulation of chromosome replication in Bacillus subtilis: marker frequency analysis after amino acid starvation. Science *172*, 159–161.

Corn, J.E., and Berger, J.M. (2006). Regulation of bacterial priming and daughter strand synthesis through helicase-primase interactions. Nucleic Acids Res. *34*, 4082–4088.

Courcelle, J., and Hanawalt, P.C. (2003). RecA-dependent recovery of arrested DNA replication forks. Annu. Rev. Genet. *37*, 611–646.

Duggin, I.G., and Wake, R.G. (2002). Termination of chromosome replication. In Bacillus subtilis and Its Closest Relatives: From Genes to Cells, A.L. Sonenshein, J.A. Hoch, and R. Losick, eds. (Washington, D.C.: ASM Press), pp. 87–95.

Dworkin, J., and Losick, R. (2002). Does RNA polymerase help drive chromosome segregation in bacteria? Proc. Natl. Acad. Sci. USA *99*, 14089–14094.

Eymann, C., Homuth, G., Scharf, C., and Hecker, M. (2002). Bacillus subtilis functional genomics: global characterization of the stringent response by proteome and transcriptome analysis. J. Bacteriol. *184*, 2500–2520.

Foti, J.J., Schienda, J., Sutera, V.A., Jr., and Lovett, S.T. (2005). A bacterial G protein-mediated response to replication arrest. Mol. Cell *17*, 549–560.

Gautam, A., and Bastia, D. (2001). A replication terminus located at or near a replication checkpoint of Bacillus subtilis functions independently of stringent control. J. Biol. Chem. *276*, 8771–8777.

Griffiths, D.J., Liu, V.F., Nurse, P., and Wang, T.S. (2001). Role of fission yeast primase catalytic subunit in the replication checkpoint. Mol. Biol. Cell *12*, 115–128.

Harwood, C.R., and Cutting, S.M., eds. (1990). Molecular Biological Methods for Bacillus (Chichester, U.K.: John Wiley & Sons).

Inaoka, T., and Ochi, K. (2002). RelA protein is involved in induction of genetic competence in certain Bacillus subtilis strains by moderating the level of intracellular GTP. J. Bacteriol. *184*, 3923–3930.

Johnson, A., and O'Donnell, M. (2005). Cellular DNA replicases: components and dynamics at the replication fork. Annu. Rev. Biochem. *74*, 283–315.

Khodursky, A.B., Peter, B.J., Schmid, M.B., DeRisi, J., Botstein, D., Brown, P.O., and Cozzarelli, N.R. (2000). Analysis of topoisomerase function in bacterial replication fork movement: use of DNA microarrays. Proc. Natl. Acad. Sci. USA *97*, 9419–9424.

Koc, A., Wheeler, L.J., Mathews, C.K., and Merrill, G.F. (2004). Hydroxyurea arrests DNA replication by a mechanism that preserves basal dNTP pools. J. Biol. Chem. *279*, 223–230.

Krasny, L., and Gourse, R.L. (2004). An alternative strategy for bacterial ribosome synthesis: Bacillus subtilis rRNA transcription regulation. EMBO J. *23*, 4473–4483.

Lee, J.B., Hite, R.K., Hamdan, S.M., Xie, X.S., Richardson, C.C., and van Oijen, A.M. (2006). DNA primase acts as a molecular brake in DNA replication. Nature *439*, 621–624.

Lemon, K.P., and Grossman, A.D. (2000). Movement of replicating DNA through a stationary replisome. Mol. Cell *6*, 1321–1330.

Lemon, K.P., Moriya, S., Ogasawara, N., and Grossman, A.D. (2002). Chromosome replication and segregation. In Bacillus subtilis and Its Closest Relatives: From Genes to Cells, A.L. Sonenshein, J.A. Hoch, and R. Losick, eds. (Washington, D.C.: ASM Press), pp. 73–86.

Levine, A., Vannier, F., Dehbi, M., Henckes, G., and Seror, S.J. (1991). The stringent response blocks DNA replication outside the ori region in Bacillus subtilis and at the origin in Escherichia coli. J. Mol. Biol. *219*, 605–613.

Levine, A., Autret, S., and Seror, S.J. (1995). A checkpoint involving RTP, the replication terminator protein, arrests replication downstream of the origin during the Stringent Response in Bacillus subtilis. Mol. Microbiol. *15*, 287–295.

Lopez, J.M., Dromerick, A., and Freese, E. (1981). Response of guanosine 5′-triphosphate concentration to nutritional changes and its significance for Bacillus subtilis sporulation. J. Bacteriol. *146*, 605–613.

Lusetti, S.L., and Cox, M.M. (2002). The bacterial RecA protein and the recombinational DNA repair of stalled replication forks. Annu. Rev. Biochem. *71*, 71–100.

Maric, C., Levacher, B., and Hyrien, O. (1999). Developmental regulation of replication fork pausing in Xenopus laevis ribosomal RNA genes. J. Mol. Biol. *291*, 775–788.

Michael, W.M., Ott, R., Fanning, E., and Newport, J. (2000). Activation of the DNA replication checkpoint through RNA synthesis by primase. Science *289*, 2133–2137.

Michel, B., Grompone, G., Flores, M.J., and Bidnenko, V. (2004). Multiple pathways process stalled replication forks. Proc. Natl. Acad. Sci. USA *101*, 12783–12788.

Milon, P., Tischenko, E., Tomsic, J., Caserta, E., Folkers, G., La Teana, A., Rodnina, M.V., Pon, C.L., Boelens, R., and Gualerzi, C.O. (2006). The nucleotide-binding site of bacterial translation initiation factor 2 (IF2) as a metabolic sensor. Proc. Natl. Acad. Sci. USA *103*, 13962–13967.

Ochi, K., Kandala, J., and Freese, E. (1982). Evidence that Bacillus subtilis sporulation induced by the stringent response is caused by the decrease in GTP or GDP. J. Bacteriol. *151*, 1062–1065.

Pages, V., and Fuchs, R.P. (2003). Uncoupling of leading- and lagging-strand DNA replication during lesion bypass in vivo. Science *300*, 1300–1303.

Renzette, N., Gumlaw, N., Nordman, J.T., Krieger, M., Yeh, S.P., Long, E., Centore, R., Boonsombat, R., and Sandler, S.J. (2005). Localization of RecA in Escherichia coli K-12 using RecA-GFP. Mol. Microbiol. *57*, 1074–1085.

Schneider, D.A., Murray, H.D., and Gourse, R.L. (2003). Measuring control of transcription initiation by changing concentrations of nucleotides and their derivatives. Methods Enzymol. *370*, 606–617.

Schreiber, G., Ron, E.Z., and Glaser, G. (1995). ppGpp-mediated regulation of DNA replication and cell division in Escherichia coli. Curr. Microbiol. *30*, 27–32.

Simmons, L.A., Grossman, A.D., and Walker, G.C. (2007). Replication is required for the RecA localization response to DNA damage in Bacillus subtilis. Proc. Natl. Acad. Sci. USA *104*, 1360–1365.

Soultanas, P. (2005). The bacterial helicase-primase interaction: a common structural/functional module. Structure *13*, 839–844.

Sung, H.M., and Yasbin, R.E. (2002). Adaptive, or stationary-phase, mutagenesis, a component of bacterial differentiation in Bacillus subtilis. J. Bacteriol. *184*, 5641–5653.

Timson, J. (1975). Hydroxyurea. Mutat. Res. *32*, 115–132.

Trautinger, B.W., Jaktaji, R.P., Rusakova, E., and Lloyd, R.G. (2005). RNA polymerase modulators and DNA repair activities resolve conflicts between DNA replication and transcription. Mol. Cell *19*, 247–258.

Vasantha, N., and Freese, E. (1980). Enzyme changes during Bacillus subtilis sporulation caused by deprivation of guanine nucleotides. J. Bacteriol. *144*, 1119–1125.

Walker, G. (1996). The SOS response of Escherichia coli. In Escherichia coli and Salmonella: Cellular and Molecular Biology, F.C. Neidhardt, R. Curtiss, III, J.L. Ingraham, E.C.C. Lin, K.B. Low, B. Magasanik, W.S. Reznikoff, M. Riley, M. Schaechter, and H.E. Umbarger, eds. (Washington, D.C.: ASM Press), pp. 1400–1416.

Wendrich, T.M., and Marahiel, M.A. (1997). Cloning and characterization of a relA/spoT homologue from Bacillus subtilis. Mol. Microbiol. *26*, 65–79.

Werner, R. (1971). Nature of DNA precursors. Nat. New Biol. *233*, 99–103.

Zhang, Z., Macalpine, D.M., and Kapler, G.M. (1997). Developmental regulation of DNA replication: replication fork barriers and programmed gene amplification in Tetrahymena thermophila. Mol. Cell. Biol. *17*, 6147–6156.

Zyskind, J.W., and Smith, D.W. (1992). DNA replication, the bacterial cell cycle, and cell growth. Cell *69*, 5–8.